AFRC 2023 Industrial Combustion Symposium
Denver, Colorado
September 25–27

Swiss-roll Autothermal Ammonia Reformer for Gas Turbine Applications

Patryk Radyjowski[1]*, David Carlson[1], Patharapong Bhuripanyo[2], Chien-Hua Chen[1], and Paul Ronney[2]

[1]Advanced Cooling Technologies, Inc., Lancaster, PA, USA

[2]University of Southern California, Los Angeles, CA, USA

*Corresponding Author Email: patryk.radyjowski@1-act.com

Abstract:

Ammonia (NH_3) is an attractive carbon-free energy carrier alternative to hydrogen (H_2) due to substantially lower storage pressure and higher volumetric energy density. Therefore, NH_3 has been considered as fuel for gas turbines for aviation or electricity generation, in which there is a requirement of substantial on-board/on-site fuel storage. However, the inherently low flame speeds of the NH_3-air mixture result in narrow flammability limits and general combustion instabilities, which make ammonia challenging to implement in conventional gas turbines. This can be alleviated by blending ammonia with small amounts of H_2, which can be generated in situ by reforming the primary ammonia fuel. With this motivation, a novel Swiss-roll style heat-recirculating fuel reformer is proposed as an upstream fuel reformer for an ammonia-fueled gas turbine system. The reforming occurs autothermally, where the exothermic reaction of partially oxidizing the ultra-rich NH_3-air mixture is used to support the endothermic reaction of breaking down NH_3 to H_2 and N_2. The Swiss-roll geometry enables extremely high thermal efficiency by minimizing heat losses and effectively recuperating the thermal enthalpy from the product stream to the reactant stream. This enables "super-adiabatic" reaction temperatures in the center of the device, leading to accelerated chemical reaction rates. Thus, the products are driven toward their equilibrium state, in which hydrogen concentration is the highest (40+%$_{mol}$), more rapidly than would be possible without recuperation. The hydrogen-rich product stream is subsequently combined with the neat ammonia supply providing a fuel-air mixture with higher flame speeds compatible with conventional gas turbine applications. This concept has been studied both numerically and experimentally. 0D kinetic and 2D Computational Fluid Dynamics simulations were used to identify the critical parameters for reforming performance and determine the optimal design space. A sub-scale Swiss-roll (6"-scale) design was additively manufactured in Inconel 718 and successfully tested over a range of flow conditions at atmospheric pressure. A wide range of rich NH_3-air mixtures were investigated for potential reforming applications. Stable reactions were sustained for mixtures as rich as equivalence ratio $\Phi = 6$. Reformate with an H_2 composition of up to 45%$_{mol}$ has been successfully generated out of neat ammonia without the use of any catalyst. Finally, the scaleup design of Swiss-roll reformers for application to MW-range gas turbines is discussed.

1. INTRODUCTION

The movement towards net-zero emissions has highlighted the need for power generation technologies utilizing carbon-free fuels such as hydrogen (H_2). Meanwhile, ammonia (NH_3) is a promising energy source for future power generation or used as an H_2 carrier. Ammonia's relatively high volumetric energy density (15.6 MJ/L) is significantly higher than difficult-to-handle cryogenic H_2 (9.1 MJ/L) and nearly three times that of compressed H_2 (5.6 MJ/L). Combined with acceptable gravimetric energy density (22.5MJ/kg), relative ease of production, transport, and storage makes it a favorable candidate as a fuel for the next generation of green gas turbines for aviation and power generation [1]. Furthermore, NH_3 is currently in use commercially as a commodity chemical, refrigerant, and fertilizer. Hence the infrastructure for its production, transportation, and distribution is already established.

Gas turbines, a substantial component of energy generation mixture, seem to be an obvious application for the emerging carbon-free fuel. However, there are several technical factors that contribute to troubled ammonia implementation. First, the chemical reaction rates of ammonia combustion are relatively slow, leading to substantially lower laminar flame speed and larger combustors required than common hydrocarbon fuels. Low laminar flame speed combined with reduced residence time dictated by the lower calorific value of ammonia leads to significant flame-holding issues. Meanwhile, the lower volumetric heat release than hydrocarbon fuels necessitates higher flow rates, further intensifying the slow reaction rates issue. Additionally, the adiabatic flame temperature is usually 100-200 K cooler than popular natural gas fuel, which interferes with turbomachinery inlet temperature requirements. Finally, NH_3-air combustion emits substantially more NO_x pollution than current state-of-the-art hydrocarbon burners. Nonetheless, there are ongoing efforts to develop direct ammonia combustors for gas turbines, such as NH_3-CH_4-H_2 fuel mixing [2], swirl-stabilized burners [3], or rich-quench-lean (RQL) staged combustion approaches [4].

The current work concentrated on an alternative approach, where NH_3 is pre-cracked upstream of the gas turbine. The reforming device can be optimized for sustaining ammonia chemistry without the need for extensive modifications to the gas turbine itself. Meanwhile, the produced reformate can be combusted directly in an H_2-targeted gas turbine or mixed with supplemental NH_3 to increase energy density, Figure 1A, while retaining the benefit of improved flame speed by blending with H_2 [1,5]. The controlled mixing of H_2-rich reformate with neat NH_3 allows for fine-tuning of the combustion characteristics, as conveyed by the effect on laminar flame velocity in Figure 1B [6]. Several studies [7,8] identified 70-30% NH_3-H_2 blend as optimal for stable combustion in gas turbines.

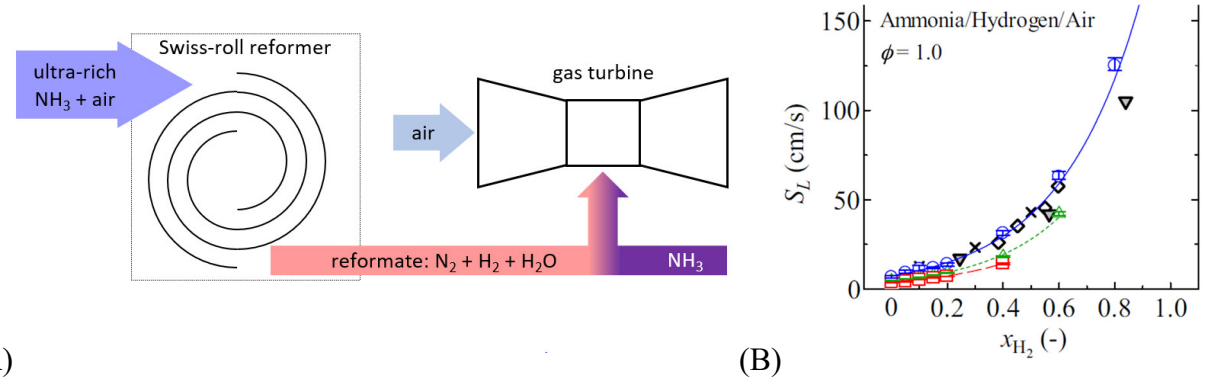

(A) (B)

Figure 1: *(A)* Simplified system schematic *(B)* Laminar flame speed for Ammonia/Hydrogen-Air at equivalence ratio (Φ) = 1 for a range of hydrogen molar fraction in fuel [6].

Most NH_3 reforming methods are based on thermodynamics, where the ultimate H_2 output is limited by either kinetic or chemical equilibrium, given a sufficient residence time. A summary of chemical equilibria for a range of temperatures and pressure is shown in Figure 2. The high operating pressure required for integration with gas turbines makes low-temperature catalyst-based solutions thermodynamically limited in conversion efficiency, as shown in Figure 2A. Therefore, using a novel heat-recirculating Swiss-roll non-catalytic thermal reformer is considered an ammonia pre-cracker for gas turbine applications. Such a device has no inherent pressure limitations as the conditions in the reaction site are usually sustained above 1000 K. A more detailed chemical equilibrium for ultra-rich ammonia combustion over a range of equivalence ratios, Figure 2B, shows substantial amounts of valuable hydrogen in the exothermic reactions range.

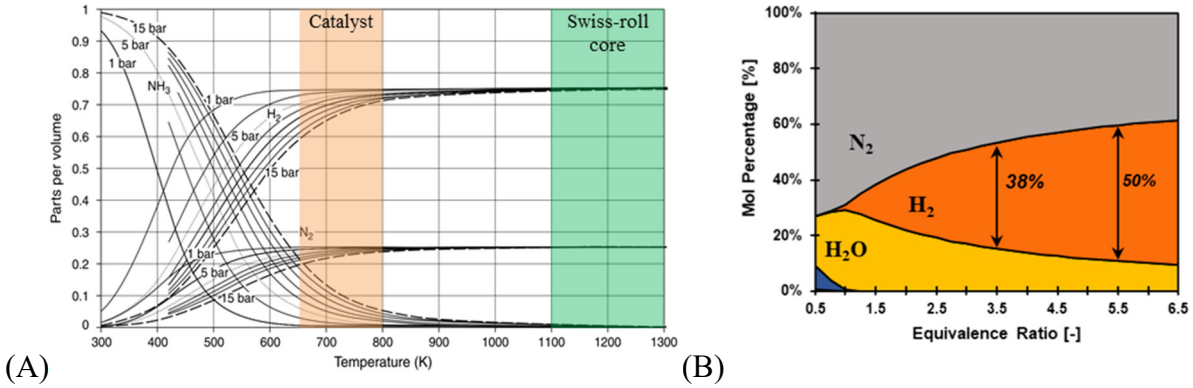

(A) (B)

Figure 2: Chemical equilibrium for: *(A)* $2\ NH_3 \leftrightarrow 3\ H_2 + N_2$ reaction at range of temperatures and pressures [9] *(B)* Products of NH_3 + air $\leftrightarrow H_2O + H_2 + N_2$ combustion for a range of equivalence ratios Φ; arrows show predicted H_2 molar fraction

Sustained operation at the most efficient conditions requires efficient use and recuperation of released thermal energy. The relevant concept of a heat-recirculating combustor was originally proposed by Weinberg [10,11]. The configuration of special interest, a Swiss-roll device, is a combustion chamber inside a spiral heat exchanger, shown schematically in Figure 3A. The cold reactants (fuel-rich mixtures of NH_3 and air) flow into the center reaction zone, where the partial oxidation reforming process occurs, while the hot products (reformate) flow out from the center through the adjacent outlet channel. The heat transfer from the hotter outlet channel to the cooler inlet channel through the spiral heat exchanger significantly increases the reactants' temperature, thus combustion temperature and reaction rates.

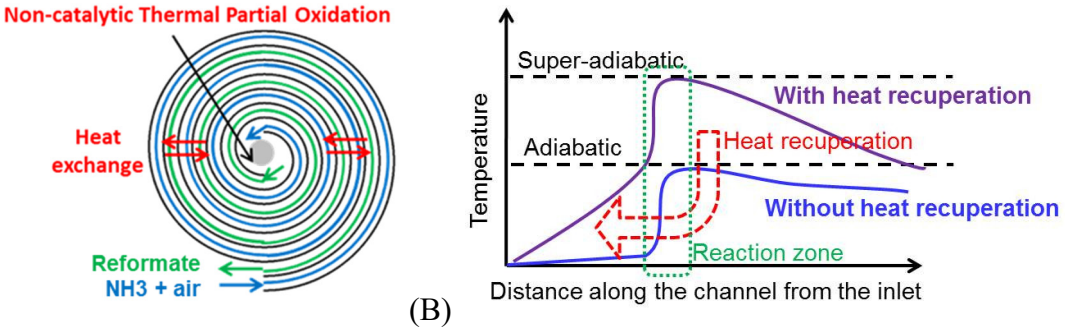

(A) (B)

Figure 3: *(A)* Schematic diagram of the Swiss-roll reformer. *(B)* Temperature profile for reaction with and without heat-recirculation.

Figure 3B further illustrates the temperature increase resulting from heat recirculation. Without heat recirculation, the reaction temperature increase is due to the exothermic reaction only, whereas with heat recirculation, the reaction zone temperature is increased by both chemical reaction and heat recirculation. The resulting reaction temperature can be higher than the adiabatic flame temperature, called "superadiabatic" flame temperature. Furthermore, the recuperated heat supplements the inevitable heat losses, extending the flammable range of various fuels and enabling the achievement of equilibrium state concentrations. The anticipated operating range for the ammonia reformer is in the ultra-rich regime, where the thermodynamic equilibrium predicts H_2 yields of up to 50% molar fraction, as shown in Figure 2B.

2. METHODS

2.1 Computational

The modeling investigation is based on a 0-dimensional perfectly-stirred reactor (PSR) combined with a 2-dimensional Computational Fluid Dynamics (CFD) study of Swiss-roll geometry. The PSR calculations characterize the important parameters affecting the reforming yield over a range of temperatures and residence times. A 0D adiabatic PSR is simulated via CHEMKIN code with GRI-Mech III detailed chemistry model [12]. Meanwhile, the CFD study explores the fuel-reforming capabilities of Inconel-718 Swiss-roll heat-recirculating combustors. The model setup includes the effects of temperature-dependent gas and solid properties. The viscous effects are modeled using Reynolds Stress Model (RSM). The outermost surface heat loss to ambient (300K) is modeled via natural convection with a 10 W/m^2K heat transfer coefficient and 0.8 external emissivity. The out-of-plane volumetric heat sink's thermal resistance model [13], as shown in Figure 4, mimics the typical experimental insulation configuration. Surface-to-surface radiation was modeled via discrete ordinates with an Inconel wall emissivity of 0.35. GRI-Mech III, Otomo's, and Song's models [14] were used for the ammonia-air chemistry model. The inlet boundary is a fixed mass-flow inlet with ambient temperature reactants.

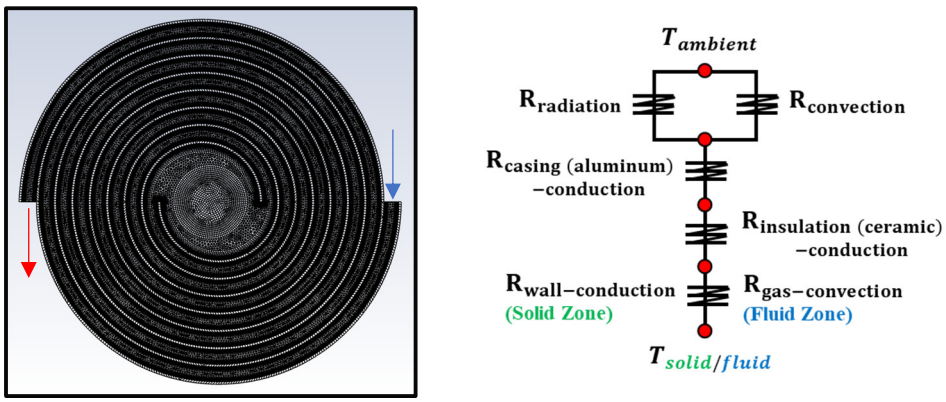

Figure 4: (*Left*) Swiss-roll base geometry and (*Right*) 1-dimensional heat loss resistance model.

The baseline geometry is a 1-ft scale, 3.5 turns cylindrical combustor with 1.25 cm channel width, 0.25 cm wall thickness, and 9.25 cm core diameter. A finned-wall variation is also included in the study, with the fin thickness comparable to that of the walls. The heights were scaled such that the effective flow's channel width remains uniform. The outlet is a specified pressure of 10 atm to represent conditions required to interface with the gas turbine.

2.2 Experimental

The experiment aimed at evaluating the operating range, measuring the reforming efficiency and validating the numerical model at pressures of 1 bar. A sub-scale 6in outer diameter Swiss-roll reformer, as presented in Figure 5, was 3D printed in Inconel 718. A 2.5-turn swirl heat exchanger included 2.5 mm wide channels separated by 1.5 mm wide walls. The core section inside the heat exchanger was 4in wide and 6in tall, with a profiled inlet at the bottom and a simple outlet at the top. The preheated reactants enter radially (Figure 5 left) and are diverted into an axial direction by a flow straightener (Figure 5 middle). This increased the residence time and helped to stabilize the ammonia combustion in the core. The hot reaction products leave the core via an adjacent channel of a spiral heat exchanger (Figure 5 right), where enthalpy is recuperated.

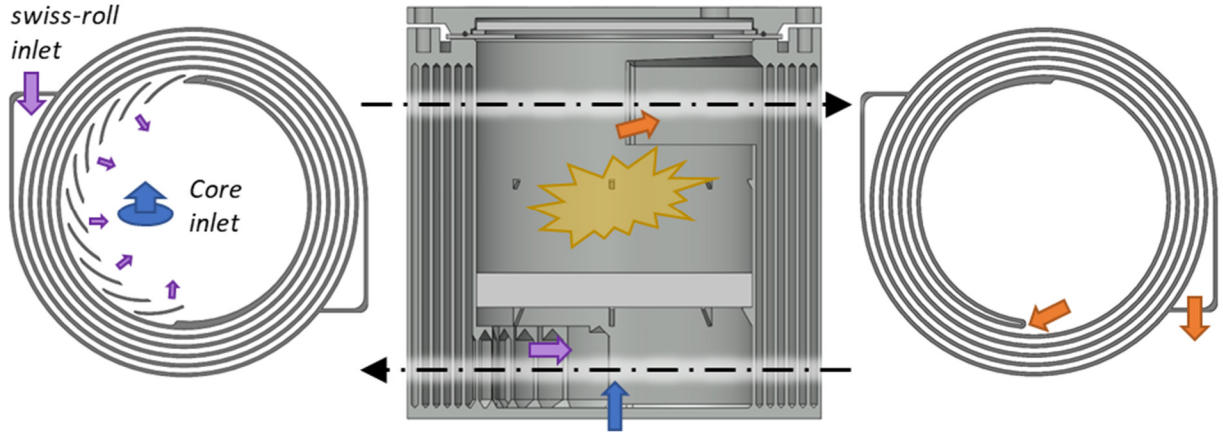

Figure 5: Internal flow pattern of Swiss-roll reformer (left) inlet swirl (middle) side cross-section of the core (right) outlet swirl.

The cross-section of the actual Swiss-roll model is shown in Figure 6A. It shows the major components, including the location of thermocouples and ignitors, main flow paths, and flow regulating components. The picture of an actual experimental reactor during operation is shown in Figure 6B.

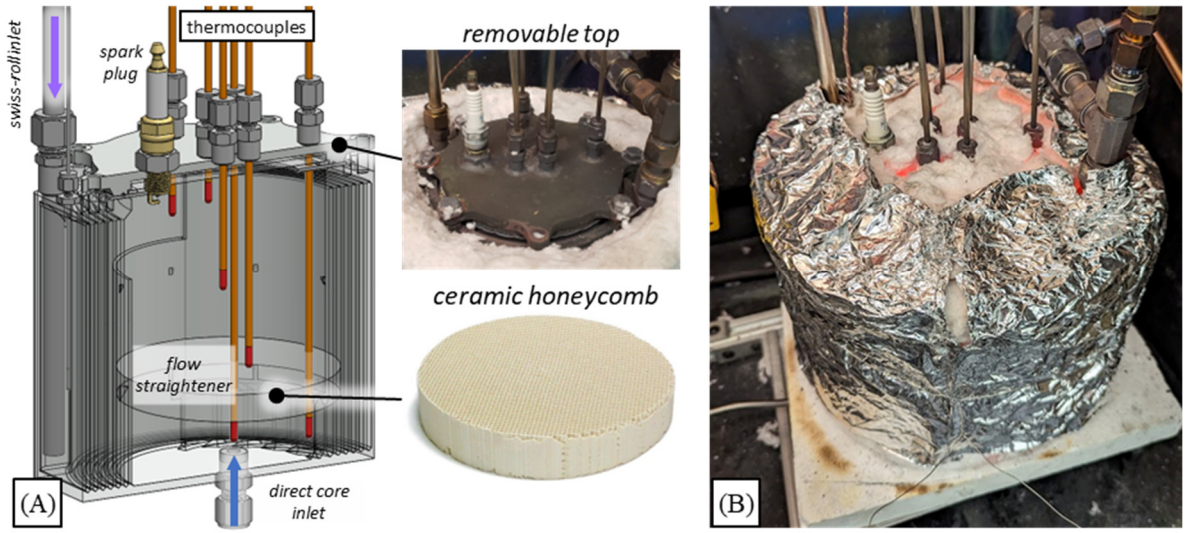

Figure 6: Experimental 6" SAAR design (A) cross-section view with major internal elements marked (B) fully assembled and under operation.

3. RESULTS AND DISCUSSION

3.1 Computational Study

The results from the 0D adiabatic PSR via CHEMKIN employing GRI-Mech III detailed chemistry are shown in Figure 7. The results suggest heightened hydrogen production with increasing ammonia concentration, temperature, and corresponding residence time. With an ammonia-rich mixture, the conversion rate becomes significant starting from 1300 K and eventually reaches a maximum at higher temperatures at a rate depending on available residence time. More detailed Otomo's and Song's chemistry models also produce similar results except for the additional effect of ammonia decomposition, which becomes significant at impractically large residence time for Swiss-roll reformer. Within a reasonable high-temperature timescale for the flame inside the Swiss-roll combustor (t_{res} ~ $1x10^{-3}$ sec - $1x10^{-1}$ sec), the results imply high-temperature flame of approximately ~2000 K will have to be sustained to achieve significant hydrogen yield. Such high value usually necessitates superadiabatic temperatures at targeted fuel-rich conditions, hence the promising role of Swiss-roll geometry.

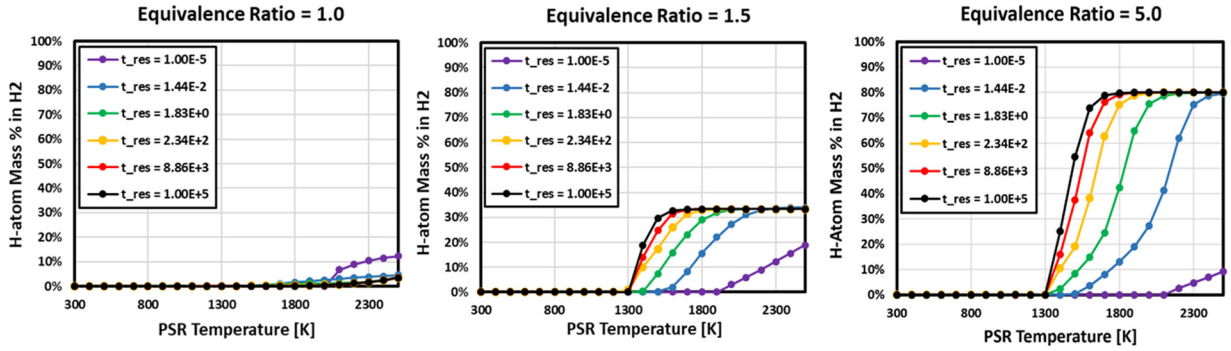

Figure 7: Hydrogen yield dependency on temperature, residence time, and mixture composition at 10atm pressure from perfectly-stirred reactor analysis with GRI-Mech III

The property called excess enthalpy [$EE \equiv (T_{max} - T_{inlet})/(T_{ad} - T_{inlet}) - 1$], quantifying the degree of heat recirculation in the system is a commonly-used design parameter for such conditions. The value can be increased by heat exchange enhancing features (added turns, fins, etc.) at the expense of increased pressure drop. Figure 8A maps the operating space of heat-recirculating reformers EE in terms of equivalence ratio and flame (PSR) temperature. Furthermore, common factors such as pressure drop, material operating temperature, and efficiency of thermodynamic processes are overlaid. This identifies a narrow design space targeted by Swiss-roll reformers with EE in the 0 to 2 range. The experimental measurements of Excess Enthalpy, Figure 8B, confirm the achievements of desired conditions.

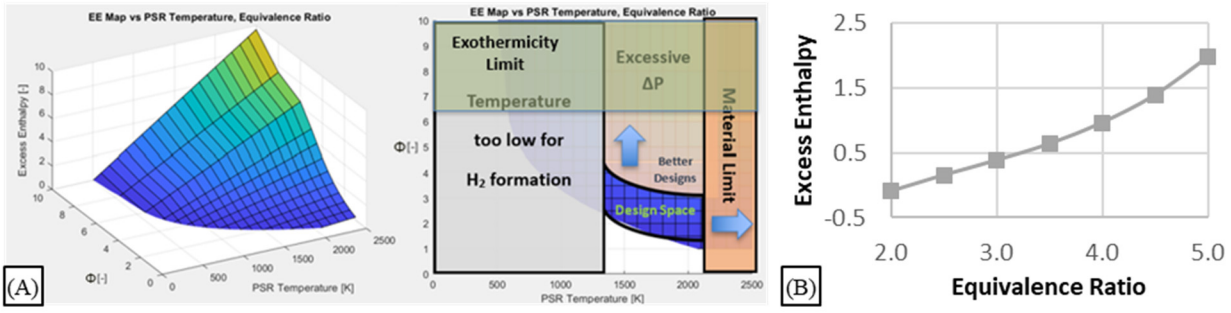

Figure 8: (A)Temperature-composition constraint diagram with Swiss-roll design considerations (B) Measured EE vs. equivalence ratio for separate fuel-air inlet operation at 70 SLPM inlet

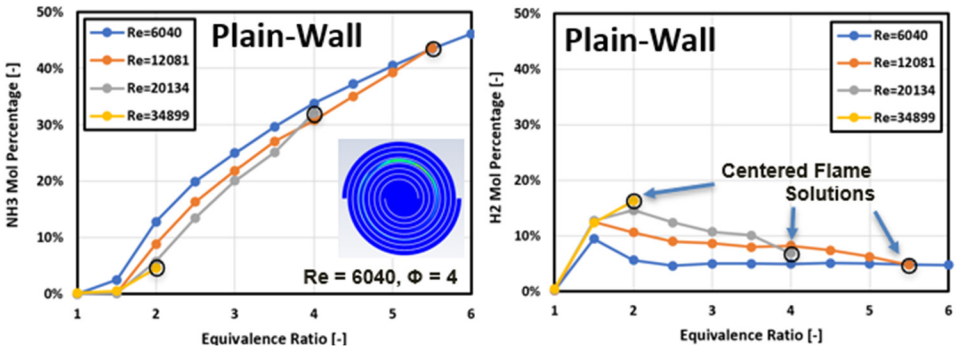

Figure 9: H-atom distributions between (*Left*) NH_3, (*Right*) H_2 at combustor outlet of 1-ft scale plain-wall Swiss-roll 3.5 turns Inconel-718 combustors (1.25 cm channel, 0.25 cm wall, 9.25 cm approximated core diameter) operating with NH_3-air mixture at 10 atm pressure.

Figure 9 above shows 2D CFD simulation results for Swiss-roll combustors at a 1-ft scale operating with fuel-rich ammonia-air mixtures at 10 atm across high flowrate cases. The primary H species composition at the combustor outlet mainly includes H_2O (not shown), H_2, and unprocessed NH_3. The amount of H_2O forms correspondingly to the number of available O atoms (solely dependent on Φ). The H_2 yield dependency on Φ follows the expected trend following the 0D PSR results. The initial rise in H_2 yield going from stoichiometric to slightly fuel-rich ($1 \leq \Phi \leq 2$) is attributed to the composition effect since the temperature is sufficiently high in this region. The following drop in H_2 yield as fuel is increased further ($\Phi \geq 2$) is due to insufficient temperature, in which the temperature becomes the primary factor determining the yield. Most of the results shown are out-of-center flames, as the combination of flowrate and composition generally produces exceedingly flammable mixtures such that the flame does not require the full recirculation benefits from the combustor. Hence the flame retreats outward along the inlet channels.

The top of Figure 10 shows the results from a similar setup but with the reaction artificially suppressed from the inlet channels. This represents the hypothetical improved design, where flashbacks are successfully suppressed. Hence the flame is allowed to reap the full recirculation benefit from the Swiss-roll combustor, leading to even higher temperatures. The resulting H_2 yield behavior again follows a bell-shaped curve, with the composition effect dominating for slightly-rich mixtures and the temperature effect ruling the ultra-rich mixtures. However, the yield instead favors low Re cases as the solution moves away from insufficient residence-time extinction limit characteristics to Swiss-roll combustors operating at a high flow rate. The extension of this thought experiment is a hypothetical finned-wall combustor design that further increases heat recirculation. The results for such configurations are presented in Figure 10 bottom. Notably, for the ultra-rich mixture cases ($4.5 \leq \Phi \leq 6$), the maximum gas temperature is practically the same (~2000 K for $\Phi \approx 4.5$, ~1860K for $\Phi \approx 6.0$) across different Re values at the same Φ. This shows the secondary effect of high-temperature residence time, favoring lower flowrate cases provided sufficiently high temperatures.

The computational study identified the potential issue of flame flashback caused by high recirculation rates leading to excessive reactivity of ammonia-air mixture. The early experiments not discussed in this paper confirmed the susceptibility for flame in the inlet channels when a premixed mixture is supplied to the inlet channel of the heat exchanger. Therefore, a modified, non-premixed fuel supply has been implemented, where only ammonia enters through the inlet channel to be preheated. Meanwhile, the air is supplied directly into the Swiss-roll core to mix with hot ammonia and combust. This configuration

arrests the reactions into the combustor center at the cost of reduced heat recirculation efficiency. Nonetheless, the recorded EE remains sufficiently high to promote efficient reforming, Figure 8.

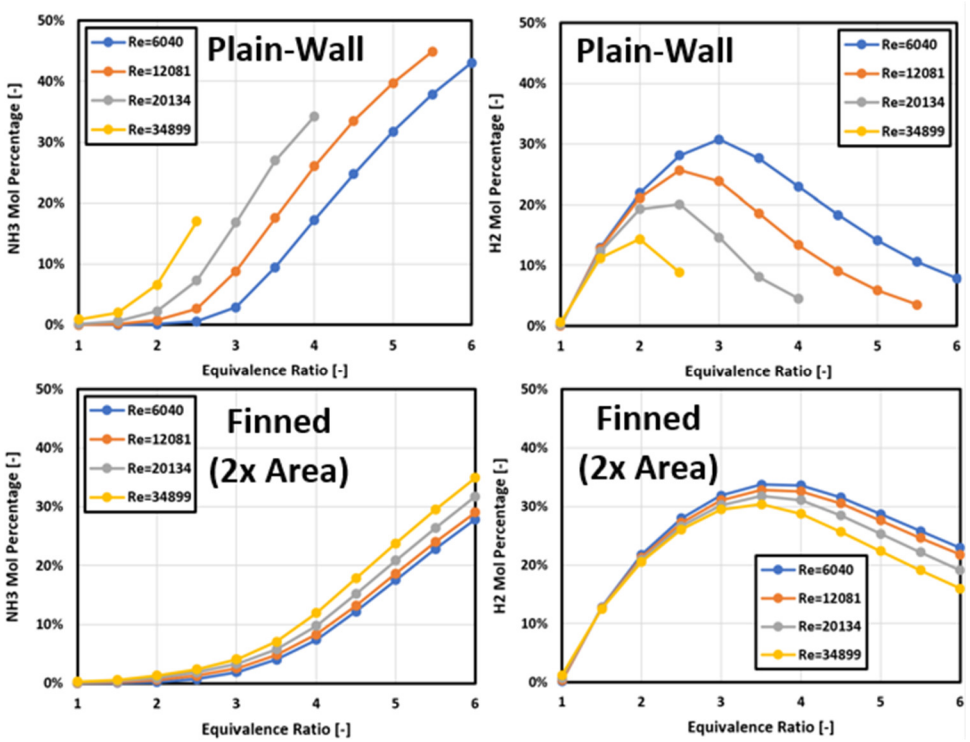

Figure 10: H-atom distributions between (*Left*) NH_3, (*Right*) H_2 at combustor outlet of 1-ft scale (*Top*) plain-wall, and (*Bottom*) finned Swiss-roll with double internal surface area, 3.5 turns Inconel-718 combustors (1.25 cm channel, 0.25 cm wall, 9.25 cm approximated core diameter) operating with NH_3-air mixture at 10 atm pressure with flame suppressed from inlet channels.

3.2 Experimental Study

The location of thermocouples and their relative steady-state readings for a range of conditions are shown in Figure 11. The temperature profile indicates the presence of stable diffusion flame inside the core for nearly all presented cases. Only the slowest flow with a stronger mixture (Re = 1.4E+4; Φ = 3.5) shows a tendency to exist near the inlet. Furthermore, the recorded temperatures remain below the operating temperature of Inconel 718, which shows the impact of material limitation on heat-recirculating combustors. Subsequent Figure 12 presents the measured hydrogen and nitrogen levels at the reformer outlet during the same set of experiments. The measured hydrogen yield for $\Phi \leq 3$ is close to the theoretical maximum indicated by thermodynamic equilibrium. The highest H_2 yield of 35% molar fraction has been achieved for $\Phi = 3.5$ and 70 $SLPM_{mix}$ inlet flow, pointing at the tradeoff between residence time and maximum temperature. The long residence time 35 $SLPM_{mix}$ case ($t_{res} \sim 1.5 \times 10^{-2}$ sec) has substantially lower H_2 content due to insufficient temperature resulting from overall low energy input into the system. Meanwhile, the performance of the fastest 105 $SLPM_{mix}$ experiment does not get hot enough (Inconel 718 limit) to overcome substantially reduced residence time. A higher temperature-tolerant material is expected to allow the high flow operation at equivalence ratios below $\Phi = 4$ while maintaining closer to the theoretical equilibrium line.

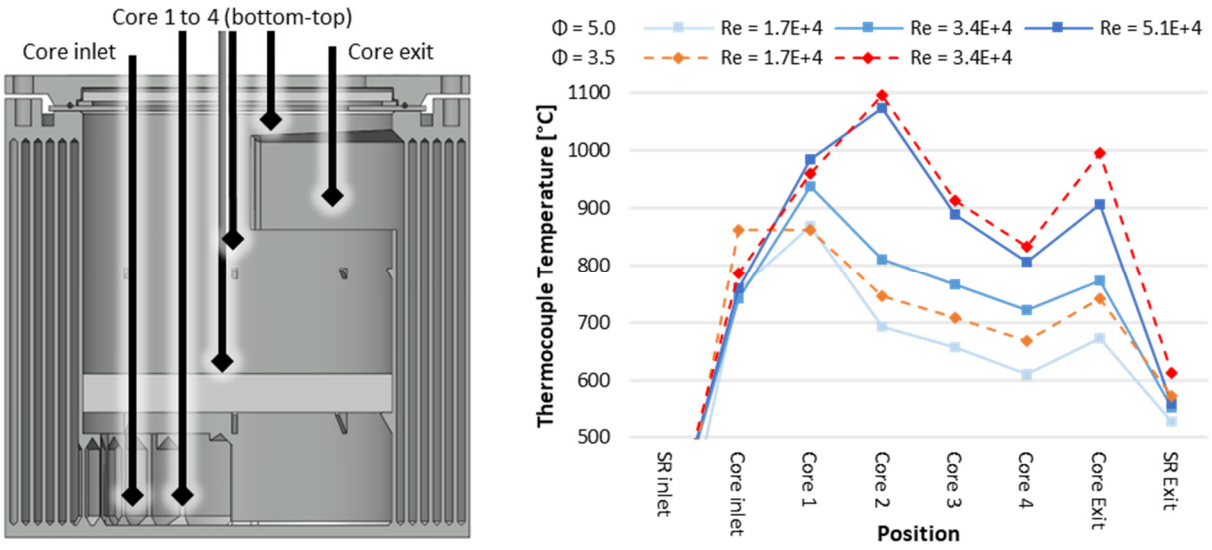

Figure 11: Swiss-roll steady-state temperature distribution for Φ = 3.5 & 5.0 and three total inlet flow rates: 35 SLPM (Re 1.7E+4), 70 SLPM (Re 3.4E+4) & 105 SLPM (Re 5.1E+4)

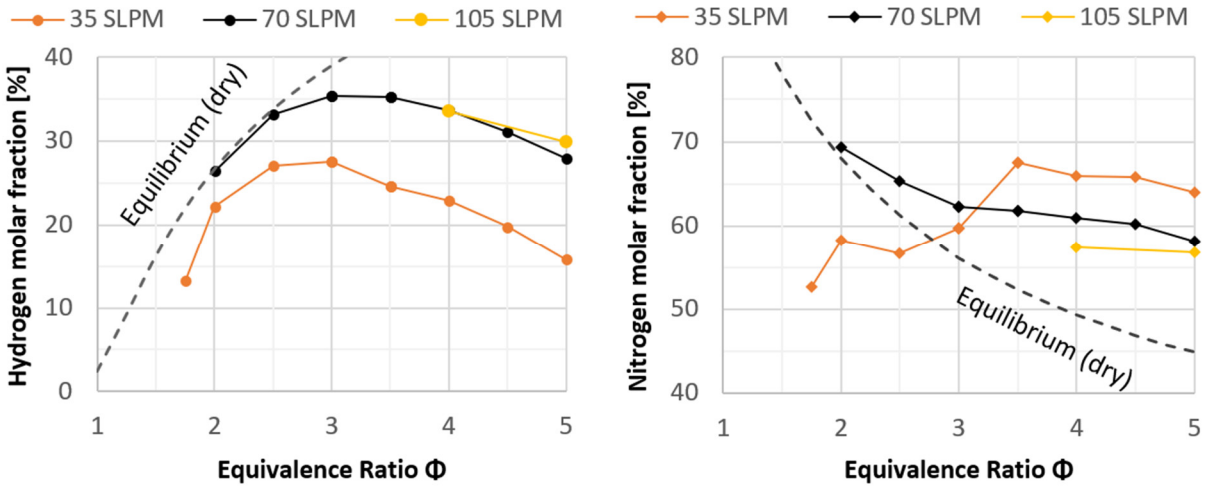

Figure 12: Hydrogen H_2 (left) and nitrogen N_2 (right) measurement of outlet reformate under a steady-state operation.

A range of reforming aids were investigated to maximize H_2 production. Figure 13B–D shows a variety of core inserts tested: empty core with a straightener (B), alumina honeycomb structure both inert and wash-coated with Nickel catalyst (C), and a pure Nickel foam suspended inside the core (D). The H_2 yields with different core inserts and the reference "Empty" case are presented in Figure 14. The introduction of uncoated ceramic ("Ceramic" case) was aimed at extending the hot zone (at-temperature residence time) for reforming reactions. The temperature profile confirmed a higher temperature in the core, but the H_2 yield has decreased slightly. Subsequently, the ceramic insert was cleaned and wash-coated with a ceria-supported Ni catalyst. It was expected that the presence of a catalyst would improve low-temperature reforming downstream of the combustion zone. The experiment ("Ceramic + Catalyst") showed an 11% lower H_2 yield with substantially depressed temperatures in the core.

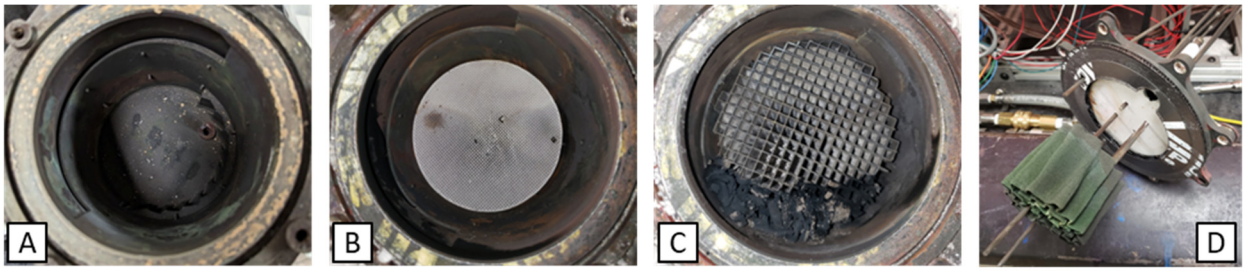

Figure 13: (A) Empty Swiss-roll core space (B) Flow straightener installed (C) ceramic catalyst base (D) Ni foam installed on the top cap, then inserted into empty space.

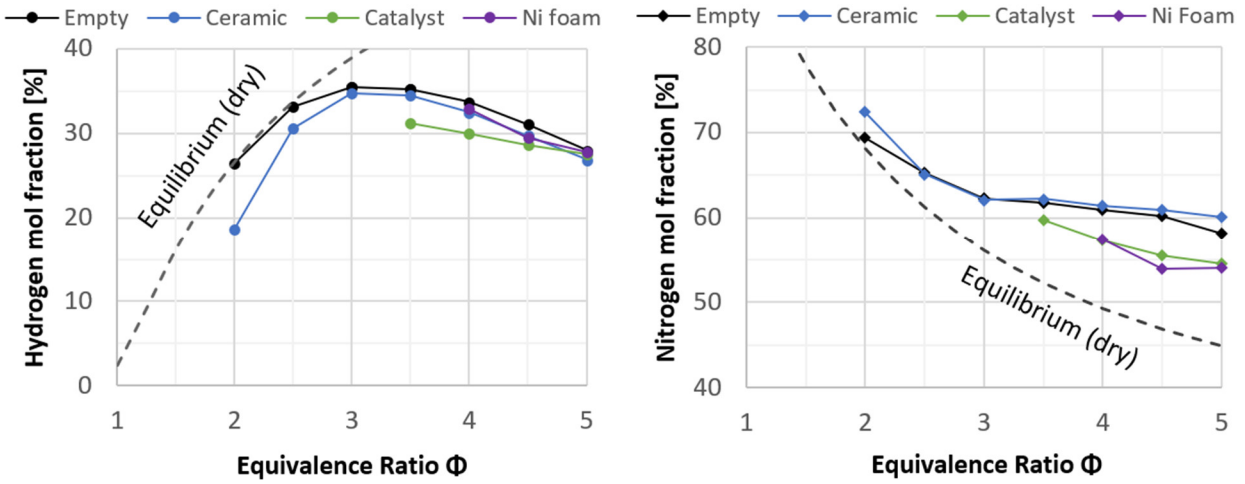

Figure 14: Hydrogen H_2 (left) and nitrogen N_2 (right) measurement for various Swiss-roll core inserts at 70 SLPM total inlet flow rate.

Notably, the N_2 mol fraction dropped below the no-catalyst cases and was closer to the equilibrium trend. Moreover, up to 0.5% O_2 was measured in the reformate at $\Phi = 3.5$, reducing to 0.1% O_2 at $\Phi = 5$. This indicates the unexpected catalyst chemistry at play. It is suspected that the strong oxygen attraction of ceria is the cause of the reduced performance. Finally, a pure Ni foam was tested without any ceramic support present – the "Ni foam" case. The overall temperature (flame position) influence was similar to the pure ceramic insert case. Despite no H_2 yield improvement compared to the base case, a similar decrease in N_2 content to the wash-coated catalyst was observed. The results point and complex chemical interactions taking place due to superadiabatic conditions and a range of compositions characteristic of non-premixed flames.

Finally, the impact of cold air directly into the core has been investigated by preheating the air stream. For reference, the core inlet flow of NH_3 was measured at around 300°C – 400°C, depending on conditions. Meanwhile, the air has been preheated to 110°C and 140° for 105 $SLPM_{mix}$ and 70 $SLPM_{mix}$ flow rates, respectively. The results are shown in Figure 15. The air preheat increased the core temperatures by approximately 100-150°C, bringing it substantially closer to Inconel temperature limits, preventing tests at $\Phi < 3.5$. A substantial 17% improvement in H_2 yield has been observed for all tested cases. Furthermore, the exceptionally high 45%$_{mol}$ H_2 at $\Phi = 4.5$ and 70 SLPM was the best-performing reforming case. The encouraging preheating results highlight the importance of efficient mixing and enthalpy management.

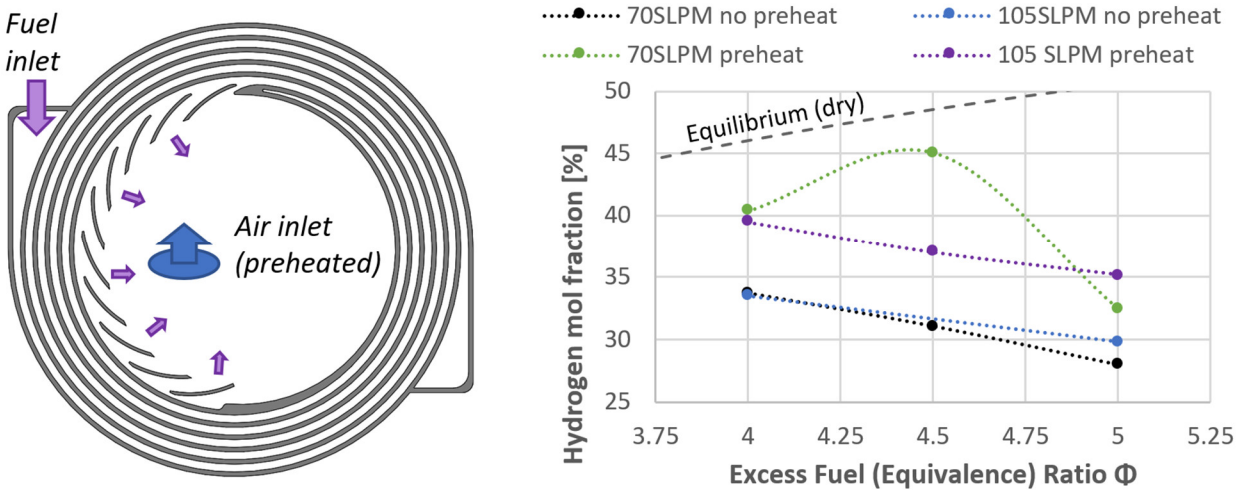

Figure 15: The influence of air preheat on H_2 yield: (left) flow configuration (right) H_2 mol fraction measurement in the reformate

3.3 Scaleup and applicability to existing gas turbine systems

Current work investigates the ammonia reformer for gas turbine utilization. The recorded performance of sub-scale 6" units operating at 1 bar allows for preliminary assessment of this technology for targeted applications. The hydrodynamic scaling laws, the necessity of maintaining heat transfer efficiency, and raising overall pressure to match that of gas turbine injectors allow scaling the experimental device's measured performance. A conservative 35%$_{mol}$ H_2 yield at the 70SLPM, Figure 12, points at a 14" Swiss-roll unit operating at 30 bar pressure capable of producing sufficient hydrogen to supply a nearly 1MW gas turbine. Using an established Solar Turbines Centaur 40 (3.5MW) unit as a reference, a quad-pack of 14" units or a single 20" Swiss-roll would be sufficient to supply this natural gas turbine with a sufficient amount of carbon-free fuel with combustion properties similar to its original fuel. The size comparison between the gas turbine package and the new Swiss-roll reforming units is shown in Figure 16. It highlights the negligible size footprint of new technology in comparison with the size of the gas turbine unit.

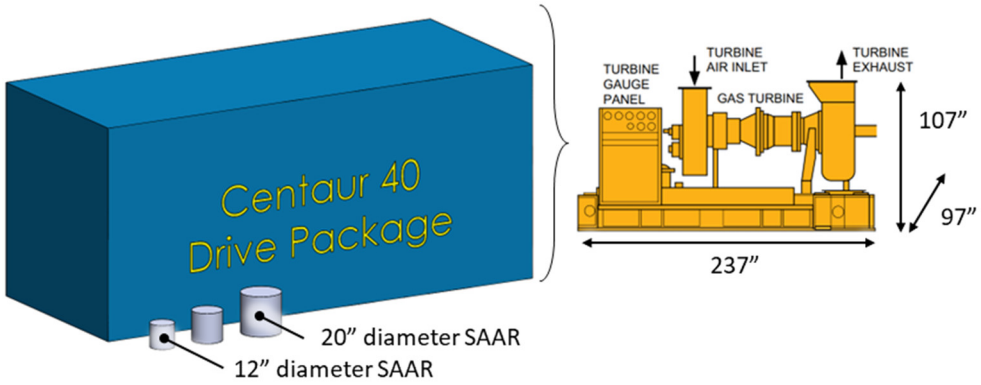

Figure 15: Size comparison between full-scale Swiss-roll devices and Solar Turbines Centaur 40 gas turbine unit [15].

4. CONCLUSIONS

Mixing hydrogen-rich reformate with ammonia is studied as a combustion augmentation method for enabling ammonia utilization in gas turbines. A novel Swiss-roll combustor has been investigated to provide the required reformate by an ultra-rich partial oxidation process. The numerical study identified the importance of Swiss-roll's excess enthalpy (EE) parameter, reaction temperature T_R, and core residence time t_{res} on expected H_2 yield. The best results are predicted for EE >2, TR > 2000 K, and t_{res} > 0.01 s. Notably, very high EE values can degrade reforming efficiency for severely insufficient T_R or t_{res} cases. The 2D study of Swiss-roll geometry supports the non-dimensional PSR findings while identifying the new issue of flame holding in the reactor core. The experimental work characterized a sub-scale 6" Swiss-roll unit's performance over a range of conditions. It has been found that a total flow rate of 70 SLPM with Φ = 3.5 produces 35%$_{mol}$ H_2, which translates to 40 $SLPM_{H2}$ out of 35 $SLPM_{NH3}$ input. The recorded level of performance allows us to predict that either a quad package of 14" units or a single 20" unit would be sufficient to power a Centaur 40 gas turbine (Solar Turbines) generating 3.5 MW. The attempted Nickel catalyst implementation failed to further increase the hydrogen yield due to encountered detrimental side chemical reactions. However, the simple air preheating enabled up to 45%$_{mol}$ H_2 at Φ = 4.5 and a total flow rate 70 SLPM. In conclusion, the amount of generated hydrogen is sufficient to augment the burning properties of ammonia for gas turbines. The presented work supports the efficacy of the Swiss-roll reformer concept as a fuel pre-cracker for gas turbine applications.

Acknowledgments

This material is based upon work supported by the U.S. Department of Energy, Office of Science, Office of Fossil Energy and Carbon Management, under Award Number DE-SC0022938.

6. References

[1] A. Valera-Medina, F. Amer-Hatem, A.K. Azad, I.C. Dedoussi, M. De Joannon, R.X. Fernandes, P. Glarborg, H. Hashemi, X. He, S. Mashruk, J. McGowan, C. Mounaim-Rouselle, A. Ortiz-Prado, A. Ortiz-Valera, I. Rossetti, B. Shu, M. Yehia, H. Xiao, M. Costa, Review on ammonia as a potential fuel: From synthesis to economics, Energy and Fuels. 35 (2021) 6964–7029. https://doi.org/10.1021/acs.energyfuels.0c03685.

[2] A.A. Khateeb, T.F. Guiberti, G. Wang, W.R. Boyette, M. Younes, A. Jamal, W.L. Roberts, Stability limits and NO emissions of premixed swirl ammonia-air flames enriched with hydrogen or methane at elevated pressures, Int. J. Hydrogen Energy. 46 (2021) 11969–11981. https://doi.org/10.1016/j.ijhydene.2021.01.036.

[3] K.D.K.A. Somarathne, S. Hatakeyama, A. Hayakawa, H. Kobayashi, Numerical study of a low emission gas turbine like combustor for turbulent ammonia/air premixed swirl flames with a secondary air injection at high pressure, Int. J. Hydrogen Energy. 42 (2017) 27388–27399. https://doi.org/10.1016/j.ijhydene.2017.09.089.

[4] D. Pugh, A. Valera-Medina, P. Bowen, A. Giles, B. Goktepe, J. Runyon, S. Morris, S. Hewlett, R. Marsh, Emissions Performance of Staged Premixed and Diffusion Combustor Concepts for an NH3/Air Flame With and Without Reactant Humidification, J. Eng. Gas Turbines Power. 143 (2021). https://doi.org/10.1115/1.4049451.

[5] J. Li, S. Lai, D. Chen, R. Wu, N. Kobayashi, L. Deng, H. Huang, A Review on Combustion Characteristics of Ammonia as a Carbon-Free Fuel, Front. Energy Res. 9 (2021).

https://doi.org/10.3389/fenrg.2021.760356.

[6] H. Kobayashi, A. Hayakawa, K.D.K.A. Somarathne, E.C. Okafor, Science and technology of ammonia combustion, Proc. Combust. Inst. 37 (2019) 109–133. https://doi.org/10.1016/j.proci.2018.09.029.

[7] M. Ditaranto, I. Saanum, J. Larfeldt, Experimental Study on High Pressure Combustion of Decomposed Ammonia: How Can Ammonia Be Best Used in a Gas Turbine?, in: Vol. 3B Combust. Fuels, Emiss., American Society of Mechanical Engineers, 2021: pp. 1–8. https://doi.org/10.1115/GT2021-60057.

[8] A. Valera-Medina, M. Gutesa, H. Xiao, D. Pugh, A. Giles, B. Goktepe, R. Marsh, P. Bowen, Premixed ammonia/hydrogen swirl combustion under rich fuel conditions for gas turbines operation, Int. J. Hydrogen Energy. 44 (2019) 8615–8626. https://doi.org/10.1016/j.ijhydene.2019.02.041.

[9] V. Hacker, K. Kordesch, Ammonia crackers, in: W. Vielstich, A. Lamm, H.A. Gasteiger (Eds.), Handb. Fuel Cells – Fundam. Technol. Appl., John Wiley & Sons, Ltd, 2003: pp. 121–127.

[10] S.A. Lloyd, F.J. Weinberg, A burner for mixtures of very low heat content, Nature. 251 (1974) 47–49. https://doi.org/10.1038/251047a0.

[11] A.R. Jones, S.A. Lloyd, F.J. Weinberg, Combustion in heat exchangers, Proc. R. Soc. London. A. Math. Phys. Sci. 360 (1978) 97–115. https://doi.org/10.1098/RSPA.1978.0059.

[12] I. V. Novosselov, P.C. Malte, S. Yuan, R. Srinivasan, J.C.Y. Lee, Chemical reactor network application to emissions prediction for industial DLE gas turbine, Proc. ASME Turbo Expo. 1 (2006) 221–235. https://doi.org/10.1115/GT2006-90282.

[13] C.-H. Chen, P.D. Ronney, Three-dimensional effects in counterflow heat-recirculating combustors, Proc. Combust. Inst. 33 (2011) 3285–3291. https://doi.org/10.1016/j.proci.2010.06.081.

[14] G.P. Smith, D.M. Golden, M. Frenklach, N.W. Moriarty, B. Eiteneer, M. Goldenberg, C.T. Bowman, R.K. Hanson, S. Song, W.C.J. Gardiner, V. V. Lissianski, Z. Qin, GRI-Mech 3.0, (2023). http://www.me.berkeley.edu/gri_mech/.

[15] “SolarAtmospheres,” Solar Turbines Centaur 40 Gas Turbine Generator Set Datasheet, (1997). https://www.solarturbines.com/en_US/products/power-generation-packages/centaur-40.html.